JOURNAL OF SYNCHROTRON RADIATION
ISSN 1600-5775

Received 9 October 2015
Accepted 14 January 2016

Edited by J. F. van der Veen

Keywords: X-ray spectrocopy beamline; multilayer grating monochromator; microspectroscopy.

The LUCIA beamline at SOLEIL

D. Vantelon,[a] N. Trcera,[a] D. Roy,[a] T. Moreno,[a] D. Mailly,[b] S. Guilet,[b] E. Metchalkov,[c] F. Delmotte,[c] B. Lassalle,[a] Pierre Lagarde[a]* and A.-M. Flank[a]

[a]Synchrotron SOLEIL, l'Orme des Merisiers, BP 48, 91192 Gif-sur-Yvette, France, [b]LPN-CNRS, Route de Nozay, 91460 Marcoussis, France, and [c]Institut d'Optique, 2 avenue Augustin Fresnel, 91127 Palaiseau Cedex, France. *Correspondence e-mail: pierre.lagarde@synchrotron-soleil.fr

Commissioned in May 2004 on the SLS machine, the LUCIA beamline was moved to the synchrotron SOLEIL during the summer of 2008. To take advantage of this new setting several changes to its design were introduced. Here, a review of the various improvements of the mechanics and, mostly, of the optics is given. Described in detail are the results of a new multilayer grating monochromator implemented on the Kohzu vessel already holding the two-crystal set-up. It consists of a grating grooved onto a multilayer (replacing the first crystal) associated to a multilayer (as a second crystal). It allows a shift of the low-energy limit of the beamline to around 500 eV with an energy resolution and a photon flux comparable with those of the previous couples of crystals (KTP and beryl).

1. Introduction

The micro-focused LUCIA beamline dedicated to X-ray fluorescence and X-ray absorption spectroscopy experiments was initially designed and installed on the SLS synchrotron to cover the energy domain from 0.8 to 8 keV by means of a two-crystal monochromator (DCM) (Flank *et al.*, 2006). In order to fully cover this domain, several couples of crystals whose 2*d* spacing matches the energy of interest have been used: beryl(1010), KTP(100), InSb(111), Si(111) were implemented on the same crystal holder of the Kohzu goniometer and these crystals could be aligned on the incoming beam by a translation of the whole assembly. Moreover, the optics of this beamline could, thanks to a pair of Kirkpatrick–Baez (KB) mirrors, focus the photon beam down to a typical value of 2.5 µm × 2.5 µm.

In 2008 LUCIA was moved to SOLEIL. In this paper, we describe the main improvements of this beamline since its transfer: on one hand, the optics has been fully replaced by new mirrors in order to solve a baseline problem at the silicon *K*-edge, the mechanics driving the KB mirrors has been changed and, on the other hand, a new multilayer grating monochromator (MGM) has been implemented. Its design is based on an engraved grating onto a multilayer substrate, associated with a flat multilayer. This hybrid technology allows us to: (i) decrease the energy limit accessible on LUCIA to open, with one single monochromator set-up, a domain spanning from 600 eV to 2.1 keV; (ii) solve the problem of flux stability due to the beam damage on the crystals (KTP and beryls) used in this energy domain, and (iii) improve the photon beam focalization for energies between 1.8 and 2.1 keV compared with InSb crystals. The full optical scheme of the beamline has, therefore, been modified, as shown in Fig. 1, and the different modifications are described below.

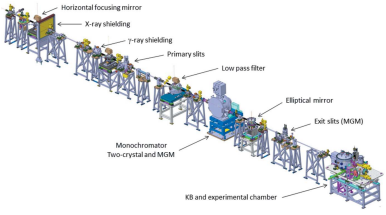

2. Optics of the beamline

The response of the beamline in the domain of energy close to the silicon *K*-edge was affected by a perturbation we attributed to a contamination of the Ni coating by Si atoms from the mirror substrate. Although this effect is quite small and most of the time, for high enough silicon concentrations, well compensated for by the I_0 normalization, it becomes unacceptable for the measurement of dilute Si samples or Si monolayers. All the mirrors were made of a polished silicon single crystal coated by 500 Å of nickel. At an incidence angle of 0.4° the substrate should not contaminate the reflected beam unless the nickel coating suffers from a diffusion of silicon atoms. This phenomenon is likely to be due to the very high affinity of nickel and silicon, and may be enhanced by the heating induced by prolonged photon irradiation. A degradation of the nickel coating, resulting in an increase of the roughness, was discarded because we did not observe any change of the focusing properties of the beamline. To solve this issue, new mirrors were made with a 5 Å-thick B_4C intermediate layer intended to prevent this interdiffusion. A control of the parameters of these new mirrors did not show any loss of their optical specifications compared with the former elements. As a consequence, the performances of the beamline in terms of photon flux and focusing properties have not been affected. Also, as expected, the spurious structure around the silicon *K*-edge has been fully suppressed, even after several months of irradiation.

The mechanics holding of the two KB mirrors has been recast. These mirrors are now mounted on translation stages which allows them to be retracted so that we can easily swap from a focused [2.5 µm × 2.5 µm with Si(111) crystals] to a full beam (2 mm × 1 mm). This modification was intended to satisfy the needs of some users for a macro- and a micro-beam on the same sample.

3. Multilayer grating monochromator

Up to now, this low-energy domain has been covered by grating monochromators using, in some cases, a separate branch aside from the existing one (Piamonteze *et al.*, 2012).

In the low-energy part of the spectral domain several weaknesses affect the user friendliness of the beamline, besides the need for a realignment of the optics following a change of crystals. KTP and, mostly, beryl crystals are fragile and hardly withstand the power of the incoming photon beam. Their reflectivity changes with time, with for instance a decrease of 50% after a few hours for beryl crystals. Moreover, beryls are natural crystals and suffer from a not perfect crystallinity which strongly affects the beam focusing. Due to the surface quality of InSb crystals, similar focalization issues are also encountered. Finally, crystal monochromators in the low-energy domain work at Bragg angles very close to 45° which kills the vertical component of the photon polarization vector and, therefore, makes the use of an Apple II undulator source less efficient.

In order to extend the possibilities of the beamline without developing a whole new branch, we have designed on LUCIA a new concept of monochromator which fulfills the following requirements: (i) it fits into the existing Kohzu two-crystal vessel which is able to reach a Bragg angle as low as 3° with an exit beam kept fixed by the cam system; (ii) it does not suffer from any radiation damage when fed by the Apple II source; and (iii) the energy resolving power is comparable with that of the Bragg monochromator, keeping in mind that the resolu-

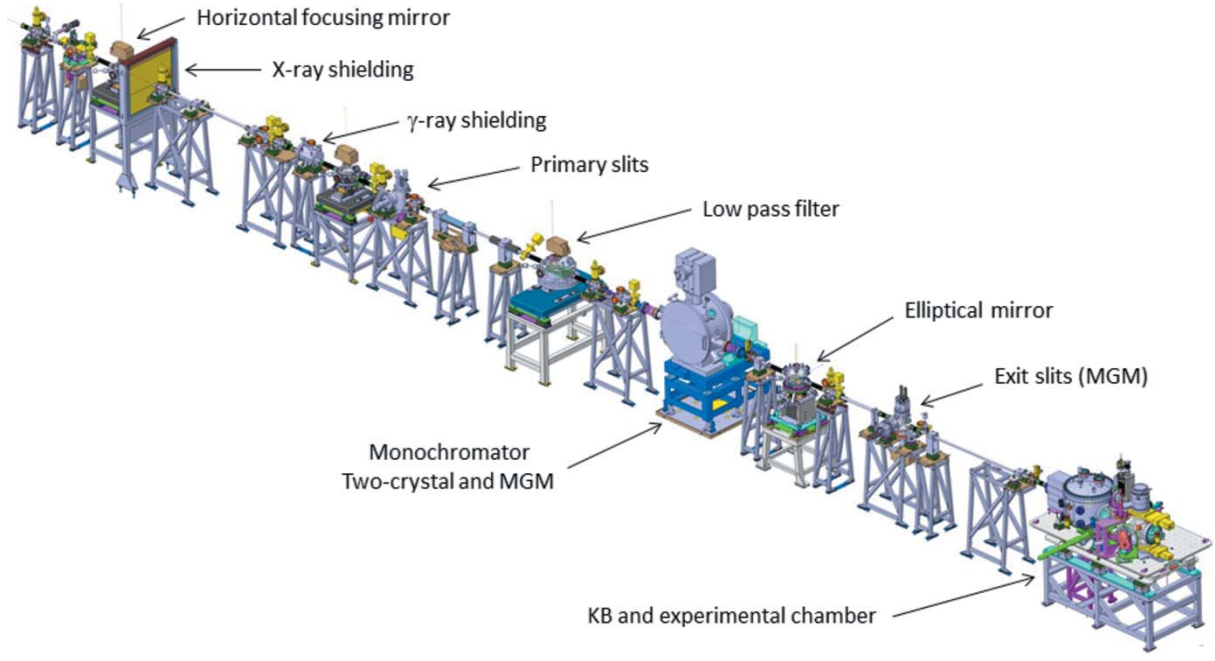

Figure 1
Layout of the LUCIA beamline at SOLEIL.

tion will be poorer anyway than the values obtained with specially designed grating systems.

3.1. Principle of the monochromator

The basic idea is to combine the good reflectivity of a multilayer and the high resolving power of a grooved grating. Since the pioneer work by T. W. Barbee (Barbee, 1989), several developments of this approach have been presented (Nakano *et al.*, 1984; Heimann *et al.*, 2005) aimed at an extension of the energy domain to higher values and using the recent improvements of the nanotechnology. An 80-pairs (Mo 25 Å, B_4C 25 Å) multilayer has a reflectivity of about 15% at 1 keV with a Bragg incident angle θ_B of *ca* 7.3° (see Fig. 2). Due to the low number of 'reflecting planes' of this multilayer, the energy resolution remains rather poor. However, when a grating with N lines per mm is grooved into this multilayer, the outcoming beam from the multilayer will be energy dispersed according to the grating law and the first order of the grating will exit at an angle $\theta_K = \theta_B - \Omega$, with $\sin(\Omega) = Nk\lambda$ [where λ is the wavelength of the photon: $\lambda = 12400/E$ (eV)]. As in the case of a two-crystal monochromator, a second, non-grooved multilayer plays the role of the second crystal in order to keep the direction of the exit beam fixed. The periodicity of this second multilayer is made slightly different from that of the first one: its wide angular acceptance still ensures a good efficiency at the energy of interest while the slight parameter mismatch will eliminate the high-order harmonics from the grating.

On the Kohzu monochromator, the grating and the multilayer are set aside from the other crystals, and the fixed angle Ω is obtained by a suitable design of the support for the multilayer. A translation of the whole DCM vessel allows to send the photon flux on each couple of crystals. When the Bragg angle θ_B is swept, the beam impinging the second multilayer changes in position but the double-cam system of the monochromator ensures a fixed position for the outgoing beam (see Fig. 3). Actually this double-cam assembly is

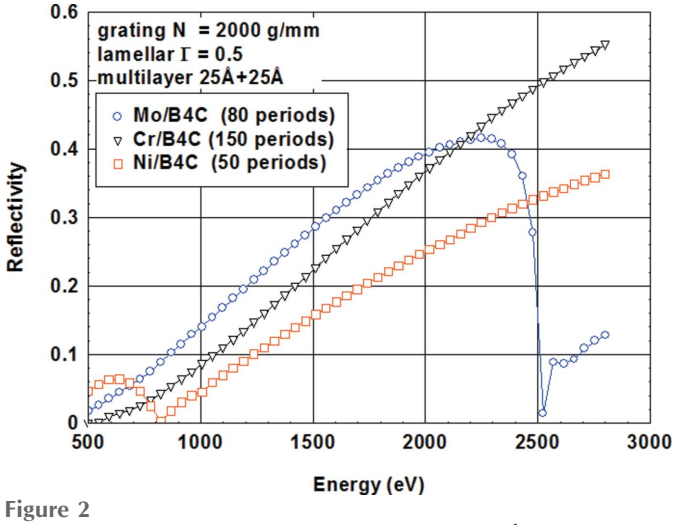

Figure 2
Efficiency as a function of energy for a 2000 lines mm^{-1} grooved pattern on different kinds of multilayers.

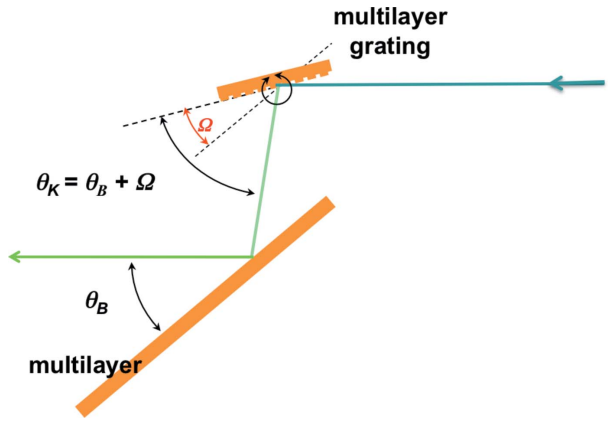

Figure 3
Optical principle of the MGM installed on the two-crystal monochromator. The only difference with the two-crystal design is the fixed angle Ω set on the multilayer holder with respect to the grating holder.

designed to keep the exit beam fixed when the two crystals are parallel. This condition is no longer satisfied here but because the angles Ω and θ_B are small the stability of the outgoing beam is preserved.

Downstream of the monochromator, an elliptical mirror focuses the exit beam onto a slit which selects, as in a classical Petersen-type grating monochromator, the energy to be used. Three widths (10, 20 or 50 µm) can be selected depending on the required flux and energy resolution. This is the only new optical element needed for the MGM installation. In order to keep the outgoing photon path fixed when swapping from the two-crystal set-up to the MGM, this mirror stays on the beam whatever the configuration of the beamline. As for the other mirrors, a 5 Å boron carbide layer has been inserted below the 500 Å nickel coating.

The energy resolution (1) is calculated with the following parameters:

ε_1, ε_2 and ε_R, which are the roughnesses of the second multilayer, the elliptical mirror and the grating, respectively.

s_1 and s_2, which are the source size (size of the photon beam in the undulator) and the size of the exit slit, respectively.

p and q, which are the source-to-monochromator distance and the mirror-to-slit distance, respectively.

Then,

$$\frac{\Delta E}{E} \propto \frac{1}{\sin(\Omega)}\left[\frac{s_1}{p} \otimes \frac{s_2}{q} \otimes 2\varepsilon_1 \otimes 2\varepsilon_2 \otimes 2\varepsilon_R\right]. \qquad (1)$$

With 3000 lines mm^{-1} and using the values for the LUCIA beamline, we expect a resolving power $E/\Delta E$ of about 4500 which stays constant over the full-energy domain because Ω is fixed.

3.2. Manufacturing process

Starting from a Mo/B_4C multilayer, a photoresist is first deposited. A groove pattern is then carved by e-beam or lithography processes. A nickel deposit is made and followed by a lifted-off step to obtain the structure of the grating drawn on the multilayer. A deep ion etching generates the final grating on the full multilayer. Once the grating has been

manufactured, the second multilayer is made with a slightly different periodicity from that of the grating in order to remove high-orders harmonics.

While in the preceding version of the beamline the vertical source of the KB mirrors was the photon beam in the undulator, this source is now the exit slit, located 3 m upstream of the vertical mirror. Actually, because the vertical size of the focus point is limited by the roughness and the slope errors of the optical elements, this change in the source distance has only a very limited effect on the vertical focusing properties (see below).

3.3. Experimental results

The grating (as a first crystal) and the multilayer have been installed on the two-crystal monochromator vessel of the LUCIA beamline, on the same holders as those used for the other crystals of the DCM. Several experiments were performed at different energies of interest in order to test the outgoing photon flux and the resolution in comparison with the previous two-crystal set-up and with grooved grating monochromators. The control command of the system remains identical provided that the 2*d* spacing corresponding to that of the multilayer is given to the software.

3.3.1. Stability and flux. Fig. 4 shows a comparison between the *K*-edge absorption spectra of magnesium measured on MgO with KTP crystals and with the MGM set-up.

The spectra are identical, the better signal-to-noise ratio of the MGM spectrum being due to the use of a four-element fluorescence detector instead of a mono-element for the KTP data. Although the two fluxes turn out to be almost the same at this energy, the response of the MGM set-up has a much higher stability: two Mg *K*-edge XANES scans recorded after four hours of irradiation between them are identical. This clearly indicates that there is no change in the throughput of the monochromator with time, in contrast to the KTP or beryl crystals. This was the first improvement we were expecting from this new technology.

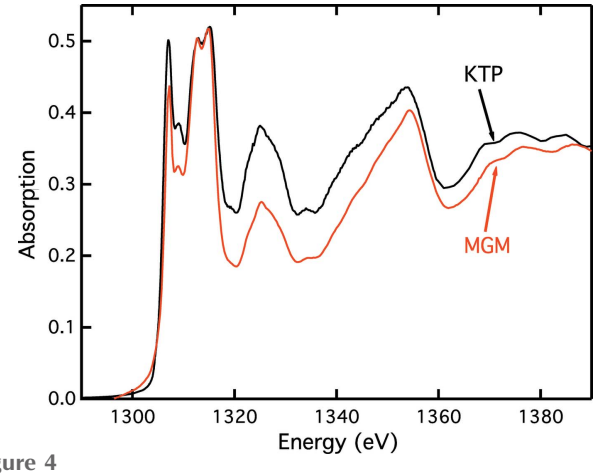

Figure 4
Comparison between the *K*-edge spectra of Mg in MgO measured with KTP crystals (black) and with the MGM (red). The energy scan parameters of the two spectra are the same, and a 20 µm slit was used for the MGM.

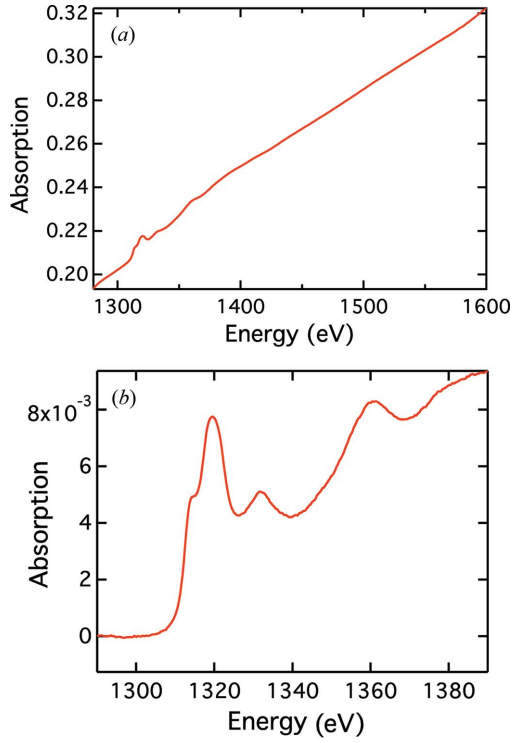

Figure 5
(*a*) Mg *K*-edge EXAFS spectrum collected in the TEY mode (one scan, elapsed time = 30 min) of a single monolayer of MgO deposited onto Ag(100). (*b*) Expanded view of the spectrum (*a*).

The output flux is actually high enough to allow surface experiments, as shown in Fig. 5, which gives the raw data obtained on a single monolayer of MgO deposited on an Ag(100) substrate.

3.3.2. Energy domain and resolution. The initial goal of the implementation of this new monochromator was to extend the energy domain covered by the beamline to lower energies and, therefore, to give access to shallow absorption edges for use in materials science, in particular the *L*-edges of the 3*d* elements. To illustrate this improvement Fig. 6(*a*) shows the Mn $L_{2,3}$-edge spectra obtained for MnO and MnO_2. They are consistent with those published using conventional grating monochromators (Morales *et al.*, 2004; Chang *et al.*, 2005; Thakur *et al.*, 2008), although the resolution is lower in the case of the MGM. Fig. 6(*b*) compares the manganese L_3-edge in MnO taken with the MGM (in red) and with the VLS plane grating monochromator of the SEXTANT beamline at SOLEIL (Sacchi *et al.*, 2013). From an analysis of the first peak at 636 eV an estimation of the instrumental resolution is possible by convolution of the VLS experimental result with a Gaussian of a given width until the best match with the MGM result is obtained. The very high resolving power of the plane grating monochromator of SEXTANT does not affect the shape of the spectrum which is governed by solid-state effects. Then we find that the contribution of the MGM is about 0.2 eV and, therefore, that the resolving power at this energy is about 3500.

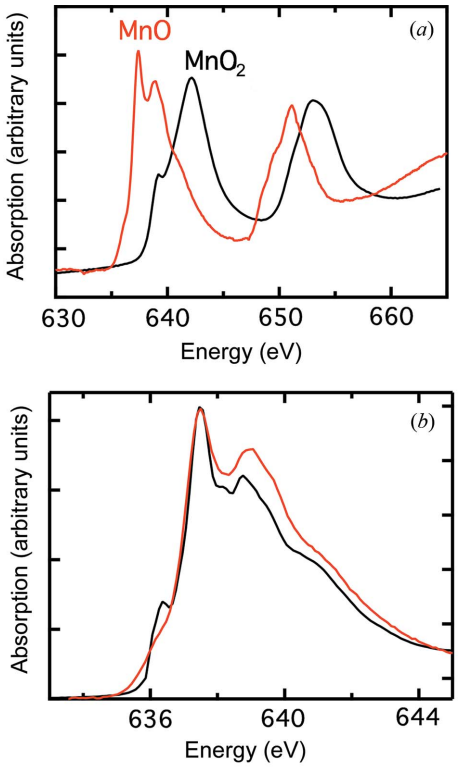

Figure 6
(*a*) Total electron yield spectrum of the manganese $L_{2,3}$-edges in MnO and MnO_2. (*b*) Mn L_3-edge in MnO taken with the MGM (red) and with a grating monochromator (black).

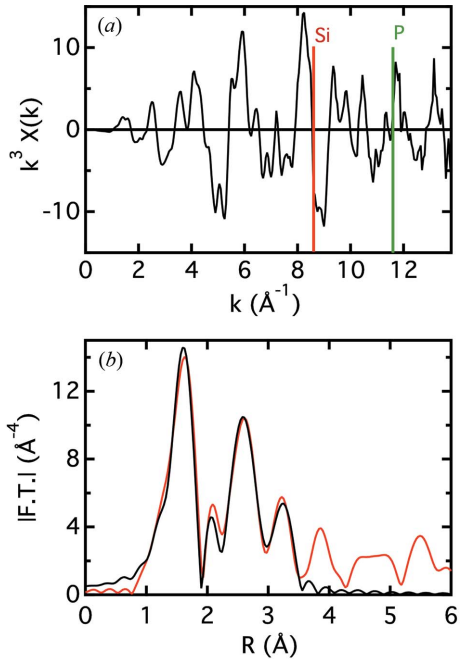

Figure 7
(*a*) $k^3\chi(k)$ EXAFS spectrum of $FeAl_2O_4$ taken with the MGM monochromator. The vertical bars are located at the position of the silicon glitch from the old mirrors and at the position of the phosphorus *K*-edge from the KTP crystals. (*b*) Comparison of experiment theory up to 3.6 Å using the crystallographic data for $FeAl_2O_4$.

To date, the lowest energy that the beamline can currently reach is slightly below 600 eV, the flux below 600 eV being limited by the efficiency of the grating and by the absorption of a 5 µm beryllium window required by the vacuum system. The replacement of this window by a diamond membrane should significantly improve the flux in this energy part of the spectrum and we then expect to reach the oxygen *K*-edge.

At high energy, the Al *K*-edge was also challenging with the two-crystal set-up. We show in Fig. 7(*a*) the $k^3\chi(k)$ EXAFS spectrum beyond the Al *K*-edge of $FeAl_2O_4$ (hercynite) which has been recorded up to 2200 eV. The bars labelled Si and P are the limits of the spectrum due to the silicon glitch from the mirrors (now corrected) and the phosphorus *K*-edge of the KTP crystals, respectively. In the low-energy region of the spectrum (below 8 $Å^{-1}$), the data taken with the two-crystal set-up and the MGM are identical. The lower part of this figure compares the Fourier transforms of the experimental data and of the theoretical model using crystallographic data of the sample. The excellent agreement assures us that the energy scan of the MGM is exact and without any distortion.

As carried out for the Mn *L*-edge spectrum, a comparison of the Al XANES taken with the two-crystal set-up and the MGM allows us to quantify the energy resolution at high energy. Fig. 8 shows this comparison and, starting from the spectrum taken with the KTP crystals, a convolution by a Gaussian function with a width of 0.55 eV matches the MGM result. Here, the contribution of the energy resolution of the KTP (around 0.2 eV) has been taken into account. Therefore, the resolving power (about 2900) appears in very good agreement with theoretical ray-tracing results (Fig. 9).

The photon flux on the sample (not focused) has also been calculated. It increases from 1.10^8 photons s^{-1} at 600 eV to 1.9×10^{10} photons s^{-1} at 2200 eV, in agreement with experimental measurements made with a silicon diode.

The focusing ability of the system has also been controlled. The source of the vertical focusing KB mirror is now the exit slit of the MGM, although it is the electron beam with the two-crystal set-up. This limits slightly the focusing properties of the beamline, which are nevertheless mainly limited by the shape errors and the roughness of the optical elements. A beamspot

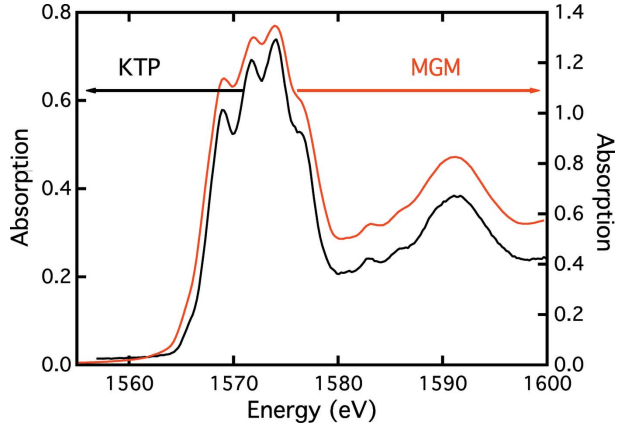

Figure 8
Near-edge spectrum of hercynite at the Al *K*-edge taken with the two set-ups.

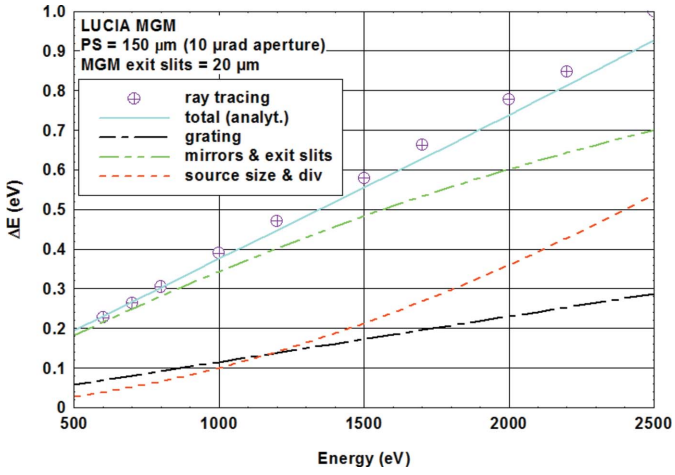

Figure 9
Theoretical calculations of the different components of the energy resolution using the parameters of the beamline (Moreno, 2016).

of about 6 µm × 6 µm has been obtained at the Si *K*-edge. This is a better result than the one obtained with InSb crystals, and a value comparable with those obtained with KTP and beryl. Therefore, the use of the MGM set-up or the two-crystal set-up will depend on the requirements of the experiment. For the study of the silicon *K*-edge EXAFS, the use of InSb crystals is more efficient and, above 2100 eV, silicon crystals are the best choice.

4. Conclusions

In the last couple of years two main improvements have been implemented on the LUCIA beamline at SOLEIL. First, we have inserted on all mirrors a 5 Å intermediate layer of B_4C between the silicon substrate and the nickel coating in order to prevent the Si/Ni interdiffusion detrimental to the baseline at the silicon *K*-edge. Then we have taken advantage of the recent improvement of nanolithography techniques to implement a multilayer grating monochromator on the two-crystal vessel. The outgoing photon flux is almost the same as the best results obtained with KTP and beryl crystals, although the stability under irradiation has been drastically improved. The resolving power of this new set-up is slightly lower than the values obtained with crystals, but this should be overcome by increasing the groove density of the grating. In order to extend the energy domain to lower energies, we plan to replace the beryllium window, which isolates the ultra-high vacuum (UHV) of the beamline to the experimental chamber at low vacuum, by a very thin diamond window. This improvement should allow the beamline to reach the oxygen *K*-edge and increase the flux at low energies.

The LUCIA beamline is now able to offer to users an energy range spanning from 600 eV to 8 keV, therefore including most of the 3*d* elements' *L*-edges, within a sample environment under low vacuum compatible with physical chemistry research. Moreover, as shown in Fig. 5, surface science experiments can be performed on a dedicated UHV vessel downstream of the main experimental chamber, at the price of a loss of the focusing properties of the beam. As the same monochromator vessel is used for the two-crystal and the MGM monochromators, there is no need for a sample transfer when the energy is changed because the beam can be kept in the same position.

Acknowledgements

We are indebted to several staff at SOLEIL: M. Thomasset for the characterization of the new mirrors, J. M. Dubuisson, P. Mercère and the Optics Group for the implementation of the MGM set-up. We acknowlege also the machine team for providing us with stable beam during the experiments.

References

Barbee, T. W. Jr (1989). *Rev. Sci. Instrum.* **60**, 1588.
Chang, W. J., Tsai, J. Y., Jeng, H.-T., Lin, J.-Y., Zhang, K. Y.-J., Liu, H. L., Lee, J. M., Chen, J. M., Wu, K. H., Uen, T. M., Gou, Y. S. & Juang, J. Y. (2005). *Phys. Rev. B*, **72**, 132410.
Flank, A.-M., Cauchon, G., Lagarde, P., Bac, S., Janousch, M., Wetter, R., Dubuisson, J. M., Idir, M., Langlois, F., Moreno, T. & Vantelon, D. (2006). *Nucl. Instrum. Methods Phys. Res. B*, **246**, 269–274.
Heimann, P. A., Koike, M. & Padmore, H. A. (2005). *Rev. Sci. Instrum.* **76**, 063102.
Morales, F., de Groot, F. M. F., Glatzel, P., Kleimenov, E., Bluhm, H., Hävecker, M., Knop-Gericke, A. & Weckhuysen, B. M. (2004). *J. Phys. Chem. B*, **108**, 16201–16207.
Moreno, T. (2016). In preparation.
Nakano, N., Kuroda, H., Kita, T. & Harada, T. (1984). *Appl. Opt.* **23**, 2386.
Piamonteze, C., Flechsig, U., Rusponi, S., Dreiser, J., Heidler, J., Schmidt, M., Wetter, R., Calvi, M., Schmidt, T., Pruchova, H., Krempasky, J., Quitmann, C., Brune, H. & Nolting, F. (2012). *J. Synchrotron Rad.* **19**, 661–674.
Sacchi, M., Jaouen, N., Popescu, H., Gaudemer, R., Tonnerre, J. M., Chiuzbaian, S. G., Hague, C. F., Delmotte, A., Dubuisson, J. M., Cauchon, G., Lagarde, B. & Polack, F. (2013). *J. Phys. Conf. Ser.* **425**, 072018.
Thakur, P., Chae, K. H., Whang, C. N., Chang, G. S., Shukla, D. K., Mollah, S. & Kumar, R. (2008). *J. Kor. Phys. Soc.* **53**, 1449.